III. 研究成果の刊行に関する一覧表

研究成果の刊行に関する一覧表

発表者氏名	論文タイトル名	発表誌名	巻号	ページ	出版年
Iwasawa K, Tanaka G, Aoyama T, Chowdhury M M, Komori K, Tanaka-Kagawa T, Jinno H, Sakai Y	Prediction of phthalate permeation through pulmonary alveoli using a cultured A549 cell-based in vitro alveolus model and a numerical simulation.	*AATEX*	18	19-31	2013
達 晃一, 星野邦広, 岩崎貴普, 曽根孝, 何 佳, 神野透人, 加藤信介	プレート吸着によるSVOCs評価法の基礎検討：DEHPの評価方法	空気調和・衛生工学会論文集	197	19-26	2013
Zhou Z., Zhao B., Kojima H., Takeuchi S., Takagi Y., Tateishi N., Iida M., Shiozaki T., Xu P., Qi L., Ren Y., Li N., Zheng S., Zhao H., Fan S., Zhang T., Liu A., Huang Y.	Simple and rapid determination of PCDD/Fs in flue gases from various waste incinerators in China using DR-EcoScreen cells.	*Chemosphere*	102	*24-30*	2014
Takeuchi S., Kojima H., Saito I., Jin K., Kobayashi S., Tanaka-Kagawa T., Jinno H.	Determination of 34 plasticizers and 25 flame retardants in indoor air from houses in Sapporo, Japan.	*Sci Total Environ*		*in press*	2014

IV. 研究成果の刊行物・別刷

ORIGINAL ARTICLE

Prediction of Phthalate Permeation Through Pulmonary Alveoli using a Cultured A549 Cell-based in Vitro Alveolus Model and a Numerical Simulation

Kokoro Iwasawa[1], Genya Tanaka[1], Takuya Aoyama[1], Mohammad Mahfuz Chowdhury[1], Kikuo Komori[1], Toshiko Tanaka-Kagawa[2], Hideto Jinno[2] and Yasuyuki Sakai[1]

[1]Institute of Industrial Science, The University of Tokyo, Tokyo, Japan
[2]National Institute of Health Sciences, Tokyo, Japan

Abstract
The animal-free prediction of inhalation toxicities in the lungs is very important concerning various low-volatile organic carbons such as phthalate. Phthalate are contained in plastics as plastisizer, easily released into environment as plastic ages, and ingested through dust. We therefore investigated benzylbutyl phthalate (BBP) permeation using an A549 cell-based lung alveolus model, in which the cell monolayers were formed on semipermeable membranes between two chambers filled with cell culture medium. With kinetic parameters obtained via these experiments, the model largely described the concentration changes in the three compartments (the apical, A549 cell, and basolateral layers) but revealed very high BBP accumulation in the alveolus cell layer at equilibrium, which did not likely reflect the in vivo situation. We therefore changed the parameter of thickness of the cell layer from 10 (cultured A549 cells) to 0.5 μm (alveoli) and the parameter of the concentration in basolateral compartment to be always zero because of the continuous perfusion of blood in vivo. After changing these parameters, the accumulation of BBP remarkably decreased, and the total permeated amount significantly increased. These results indicated that various parameters and assumptions should be changed to overcome the limitations and/or properties of existing culture models to improve the predictive accuracy of the system when using in vitro cell-based tissue models and numerical simulations to predict health hazards in humans.

Key words: *in vitro, phthalate, alveolus, Numerical model*

Introduction

Various phthalic acid esters (PAEs) have been widely used as plasticizers in a variety of consumer products and household industries (Autian, 1973; Peakall, 1975). However, phthalates are not chemically bound to the plastic polymer matrix; they can be released from products, after which they can migrate into the external environment (Giam *et al.*, 1978). It is reported that PAEs influence the metabolism of hormones involved in reproductive and developmental processes in animals (Ema *et al.*, 2000; Pan *et al.*, 2006; Salazar *et al.*, 2004; Van Meeuwen *et al.*, 2007). On assessing the effects of dibutyl phthalate (DBP) and benzylbutyl phthalate (BBP) on transactivation of the estrogen receptor and breast cancer cell growth in vitro, it was found that they were estrogenic. BBP is one of the longer phthalate molecules, and its metabolites include monobutyl phthalate (MBuP) and monobenzyl phthalate (MBeP). BBP has wide application as a plasticizer in the polymer indus-

try to improve flexibility, workability, and general handling properties; approximately 80% of all phthalates are used for this purpose (IARC, 2000). Therefore, BBP is found in a variety of products, including building materials, vinyl gloves, artificial leather, and adhesives. Since it is not commonly used in plastic toys, and thus, exposure to BBP through this route is low in infants and children (European Chemicals Bureau, 2007). However, it was suggested that ingestion of dust is a significant source of BBP exposure in young children (Wormuth *et al.*, 2006), and the source of dust is most likely building materials (Bornehag *et al.*, 2005); therefore, inhalation is the primary route of exposure to BBP.

Because of the difficulties in establishing simple in vitro pulmonary exposure systems, animal models are mainly used for toxicity tests for nanoparticles, gaseous compounds, or samples. From the standpoint of animal protection, the number of animals sacrificed in animal-based experiments must be reduced, and from the viewpoint of species differences between human and animals, it is still controversial to determine the toxicity of agents in humans on the basis of results in animal studies; thus, toxicity is generally tested using cells of human origin. Several in vitro respiratory cell systems, including static culture dishes (Patel *et al.*, 1990), dishes on tilting platforms (Dumler *et al.*, 1994; Guerrero *et al.*, 1979; Nikula *et al.*, 1990), rotating flasks (Banks *et al.*, 1990; Pace *et al.*, 1969), roller bottles (Bolton *et al.*, 1982), bubbling gas through cell suspensions (Konings, 1986), and gas permeable membranes with culture medium above the cells and gas flow beneath them (Alink *et al.*, 1980; Cheek *et al.*, 1988), have been proposed. However, it is impossible to conclude whether these systems completely mimic the in vivo situation.

In this study, we established a three-compartment model to clarify the dynamics of phthalates around the alveolar epithelial cell layer and predict the permeation and accumulation of phthalate in vivo in combination with a numerical simulation method. Although it is important to determine the toxicity associated with exposure via inhalation, in vitro research on the toxicity of phthalate and its translocation in the pulmonary system using culture inserts (Shimizu *et al.*, 2004; Komori *et al.*, 2008) has not been reported. We focused on the toxicity of BBP and its metabolites MBuP and MBeP and measured the permeation of BBP through an alveolar epithelial cell layer formed on a culture insert containing a polyester membrane to divide the apical and basal compartments. The apical compartment mimics the air in alveoli, and the basal compartment mimics pulmonary intravenous blood. Even in this system, inappropriate parameters concerning the thickness of the cell layer and the concentration of the chemicals in the basal compartment were present. To mimic the in vivo situation, we therefore changed these inappropriate parameters to elucidate the dynamics of BBP in and around alveolar epithelial cell layers.

Materials and Method

Cell culture and medium

A549 cells (ATCC® CCL-185™), which is human alveolar basal epithelial cells, and HepG2 cells(ATCC® HB-8065™), which is Human hepatocellular liver carcinoma cell line were obtained from Riken Gene Bank (Tsukuba, Japan). The cells were cultured in Dulbecco's Modified Eagle's Medium (DMEM; WAKO, Japan) supplemented with 10% fetal bovine serum (FBS; HyClone Laboratories, Inc., Waltham, MA, USA), 20 mM hydroxyethylpiperazine-*N'*-2-ethanesulfonic acid (HEPES; Dojindo, Kumamoto, Japan), and 1.0% antibiotics (A.A., Invitrogen, Drive Rockville, MD, USA). The solution of 0.25% trypsin and 0.02% EDTA in phosphate-buffered saline (PBS) was used for the cell culture passaging.

Measurement of cellular carboxylesterase (CES) activity

Diester phthalate is degraded into mono phthalate and alcohol in vivo by CES, which is present in all epithelial cells. The *p*-nitrophenyl acetate assay was performed to estimate CES activity in A549 cells based on the *p*-nitrophenol concentration produced from *p*-nitrophenyl acetate by CES (Hosokawa *et al.*, 2002). The HepG2 human hepatocyte cell line has abundant endogenous CES (Ross *et al.*, 2012); therefore, CES activity was compared between A549 and

HepG2 cells. The cells were suspended in PBS in a 15-mL tube and sonicated for 15 min. After centrifugation at 7100 rpm for 30 min, the protein concentration of the supernatant was measured, and a solution containing 20 μg/mL protein was prepared. In a 96-well plate, 100 μL of the solution was added to each well and maintained for 30 min at 37°C. Then, 100 μL of 200 mM *p*-nitrophenyl acetate was added to each well of the plate, incubated for 30 min; and the resulting amount of *p*-nitrophenol produced was measured (λ = 405 nm) using a spectrophotometer (MPR-4Ai, Tosoh, Co., Japan) to determine the level of CES activity in the cells.

Cytotoxicity assay

Chemical toxicities in A549 cells were quantitatively examined using the acid phosphatase (AP) assay, which determines the number of living cells based on AP activity(Yang *et al.*, 1996; Martin *et al.*, 1993). After exposing A549 cells to phthalate for the specified times, the cells were carefully rinsed twice with PBS to remove any dying or loosely attached cells. The cells were then exposed to 0.25 M acetate buffer solution (pH 5.5) containing 10 mM *p*-nitrophenol phosphate (Wako) as a substrate for acid phosphatase and 0.01% Triton X-100 as a cytomembrane destruction reagent for 2 h at 37°C in an incubator; the resulting *p*-nitrophenolate produced was measured using an MPR-4Ai spectrophotometer (λ= 405 nm) to determine AP activity in the cells remaining on the membrane surfaces. The % viability *R* was determined using the following equation:

$$R = 100 \times \frac{A_S - A_0}{A_C - A_0},$$

where A_s and A_c are the absorbance values after phthalate exposure and of the medium only, respectively, and A_0 is the control absorbance value.

Formation of an A549 cell layer on a membrane culture insert

After being coated with a collagen solution containing 10% collagen (Cell matrix Type I-P, Nitta Gelatin, Osaka, Japan) and exposed to 1 mN HCl in Milli-Q water for 1 h in the refrigerator, a polyester membrane culture insert with a culture a culture surface area of 1.0 cm^2 and a pore size of 0.4 μm (Transwell 3460, Coster, Cambridge, MA, USA) was washed with culture medium, and A549 cells were seeded at a density of 5.0×10^4 cells/cm^2 onto the insert. The level of confluence of the cell sheet was determined by measuring its transepithelial electrical resistance (TEER), reflecting the function of tight junctions, using a Millicell-ERS (Millipore Corp., Bedford, MA, USA), and the time course formation of a cell layer was assessed. The TEER value gradually increased over time and reached a steady state at approximately 45 Ω·cm^2 by the 7th day. Therefore, A549 cells were cultured for 7 days in subsequent experiments.

Measurement of BBP and its two metabolites in culture medium

The phthalates examined in this study are listed in Figure 1; three major phthalates (DEHP, DBP, BBP) are widely used as plasticizers, and 3 monophthalates [mono (2-ethylhexyl) phthalate (MEHP), MBuP, and MBeP] are metabolites of the three phthalates listed in Figure 1. The standard solutions prepared for all six aforementioned phthalates and all special grade chemicals were purchased from WAKO Pure Chemical Industries, Ltd. Japan.

The A549 cells monolayer was formed on a polyester membrane as described previously. BBP was once mixed with FBS, subsequently mixed with DMEM containing FBS, HEPES, and antibiotics, to form DMEM-10% FBS-2%HEPES-1% antibiotics solution. Then, 1–10 mM BBP dissolved in culture medium was added to the culture insert (apical side; Ap) cultured with A549 cells, or 0.33–3.3 mM BBP was added to the well under the culture insert (basolateral side; BL). After 48 h, 50 μL culture medium was taken from each compartment and then mixed with 50 μL acetonitrile. To separate the supernatant from precipitated proteins and cell debris, the mixtures were centrifuged at 4000 rpm for 10 min. The concentrations of phthalate and its metabolites in the supernatants were measured by HPLC (HIC-6A, Shimazu, Japan) with a reverse-phase column (Xbridge Shield RP18, Waters, USA). The measurement conditions followed the manufacturer's recommendations. The eluent was acetonitrile:

water:formic acid (15:85:0.085 by volume) with a flow rate of 1.2 mL/min, and the excitation and emission wavelengths were 254 nm.

For the measurements of time-dependent BBP concentrations, A549 cells were seeded at a density of 5.0×10^4 cells/cm^2 onto a 10-cm tissue culture dish or culture inserts (Costar 3460, Coster, Cambridge, MA, USA) and incubated for 7 days to permit the formation of a monolayer on the bottom of the dish. The concentration of BBP in the culture medium was 10 mM for the cells cultured in the 10-cm dish, and the BBP concentration in the medium was measured by HPLC at least once per day.

Results and Discussion

CES activity of A549 cells

The *p*-nitrophenyl acetate assay was performed to estimate CES activity in A549 and HepG2 cells based on the *p*-nitrophenol concentration produced from *p*-nitrophenyl acetate by CES. The concentration of *p*-nitrophenol was measured for 5 h, and the results are shown in Fig. 2. The concentration of *p*-nitrophenol increased over time and reached saturation at approximately 3 h. Although the *p*-nitrophenol level in A549 cells was significantly lower than that in HepG2 cells, its concentration in A549 cells was considerable, indicating that CES activity in these cells is indispensable. Because CES de-

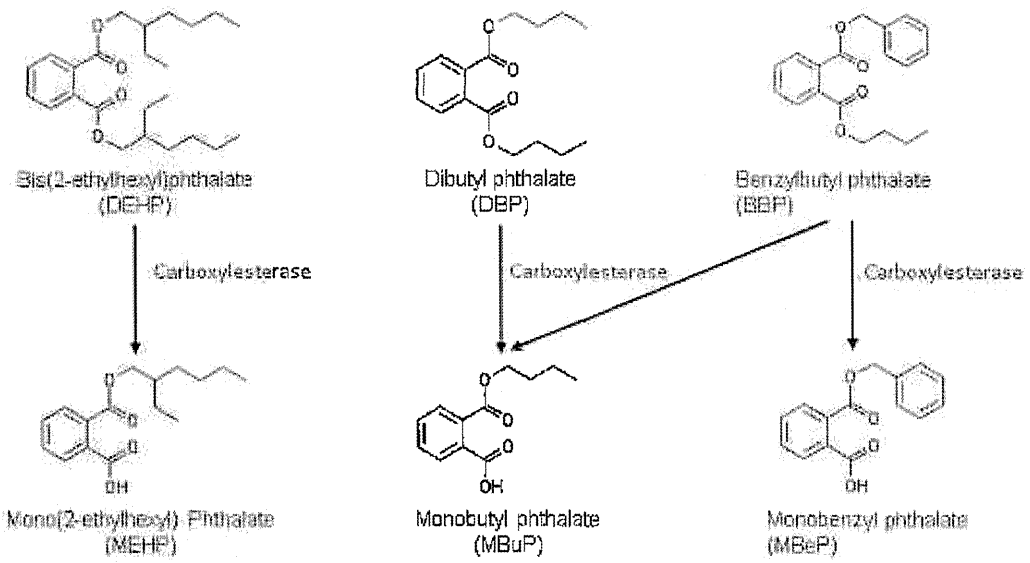

Figure 1 Phthalates examined in this study.
Three monophthalates are metabolized from the three presented phthalates.

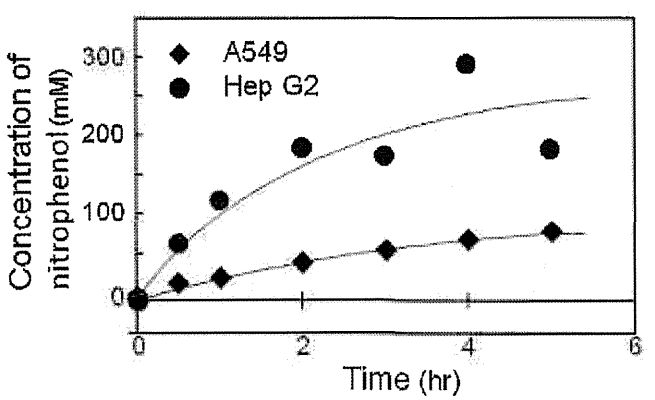

Figure 2 The concentration of p-nitrophenol metabolized from p-nitrophenyl acetate by A549 (◆) and HepG2 cells (●). Solid lines are the fitted line by least square approximation.

grades diester phthalates into monoesters, even if only a diester phthalate such as BBP was added to the cells, its monoester metabolites may exist. This result prompted us to investigate the presence of BBP and monoester phthalates such as MBuP and MBeP.

Cytotoxicity of BBP and its two metabolites MBuP and MBeP

The toxicity of BBP and its metabolites MBuP and MBeP in A549 cells at 48 h was measured by the AP assay, and the dose-response curves are presented in Fig. 3. T-test values between BBP-MBeP, BBP-MBuP and MBeP-MBuP are 0.046, 0.015 and 0.68, respectively. A549 cell viability decreased as the concentration of BBP increased. By contrast, the A549 cell viability did not decreased in the presence of MBuP and MBeP at concentrations less than 3 mM, and their viability decreased only in the presence of MBeP and MBuP at enormously high concentrations of 10 mM. It was revealed that the toxicity of BBP was higher than that of MBeP and MBuP, and both metabolites had remarkable lower toxicity than their original chemical on a molar basis. In terms of chemical structures of BBP and its two metabolites as shown in Fig. 1, BBP lacks the hydroxy group possessed by both monoesters and is considered more hydrophobic than MBuP and MBeP. In Fig. 3, the result is consistent with the principle that hydrophobic compounds are generally more toxic than hydrophilic compounds (Vesterkvist *et al.*, 2012).

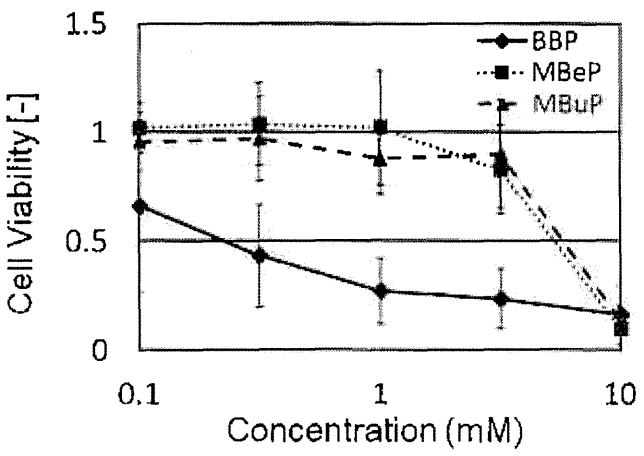

Figure 3 Dose-response curves of benzylbutyl phthalate (BBP, ◆), monobenzyl phthalate (MBeP, ■), and monobutyl phthalate (MBuP, ▲) in A549 cells 48 after phthalate was loaded into the culture medium.

Formation of two metabolites from BBP and their permeability through A549 cell layers

Medium containing BBP at one of three different concentrations (1.0, 3.2, or 10 mM) was initially added to the Ap side of the culture inserts, or medium containing 0.33, 1.1, or 3.3 mM BBP was added to the BL side. The average concentrations of BBP were 0.25, 0.79, and 2.5 mM for the three concentrations, respectively, regardless of whether BBP was added to the Ap or BL side. These average concentrations are based on the assumption that BBP is homogenously dispersed in the Ap and BL sides without the cell layers. In all cases and compartments, the concentration of MBuP was approximately 0.1 mM, which was higher than that of MBeP, indicating that MBuP was more commonly produced as a metabolite than MBeP. This finding has also been reported previously in vivo (Nativelle *et al.*, 1999).

At the same time, in all cases, the concentration of BPP was much higher than that of MBuP and MBeP in all compartments and was more than 10-fold higher in the concentration range of 1–10 mM (average, 2.5 mM). In addition, it was found that the toxicity of MBuP and MBeP was far lower than that of BBP in this study. Considering these results, we concluded that the concentrations of the BBP metabolites are negligible in the subsequent numerical simulation.

The BBP concentrations were almost identical on the Ap and BL sides 48 h after BBP was loaded on the BL side. Meanwhile, the concentration of BBP was 3~4 -fold higher on the Ap side than on the BL side when BBP was initially loaded on the Ap side. In addition, the permeability of BBP was higher when high concentrations of BBP were loaded on the Ap side. With these results, it was considered that the transport rate of BBP from the pulmonary alveoli to the blood side is minuscule (or BBP is being antiported), whereas that in the opposite direction is relatively high.

Construction of a compartment model and determination of its parameters from the permeation experiments

To summarize the above results, BBP is degraded to monophtalate MBuP and MBeP by CES, and the level of CES activity in human pulmonary epithelial A549 cells is not as high as that in human hepatocyte HepG2 cells but is not negligible (Fig. 2). Furthermore, BBP applied to A549 cells is metabolized to MBuP and MBeP, but the concentration of the metabolites are relatively low (Fig. 4). At the same time, the toxicities of these monoesters are significantly lower than that of BBP (Fig. 3); therefore, we concluded that the effect of MBuP and MBeP could be negligible for further analysis.

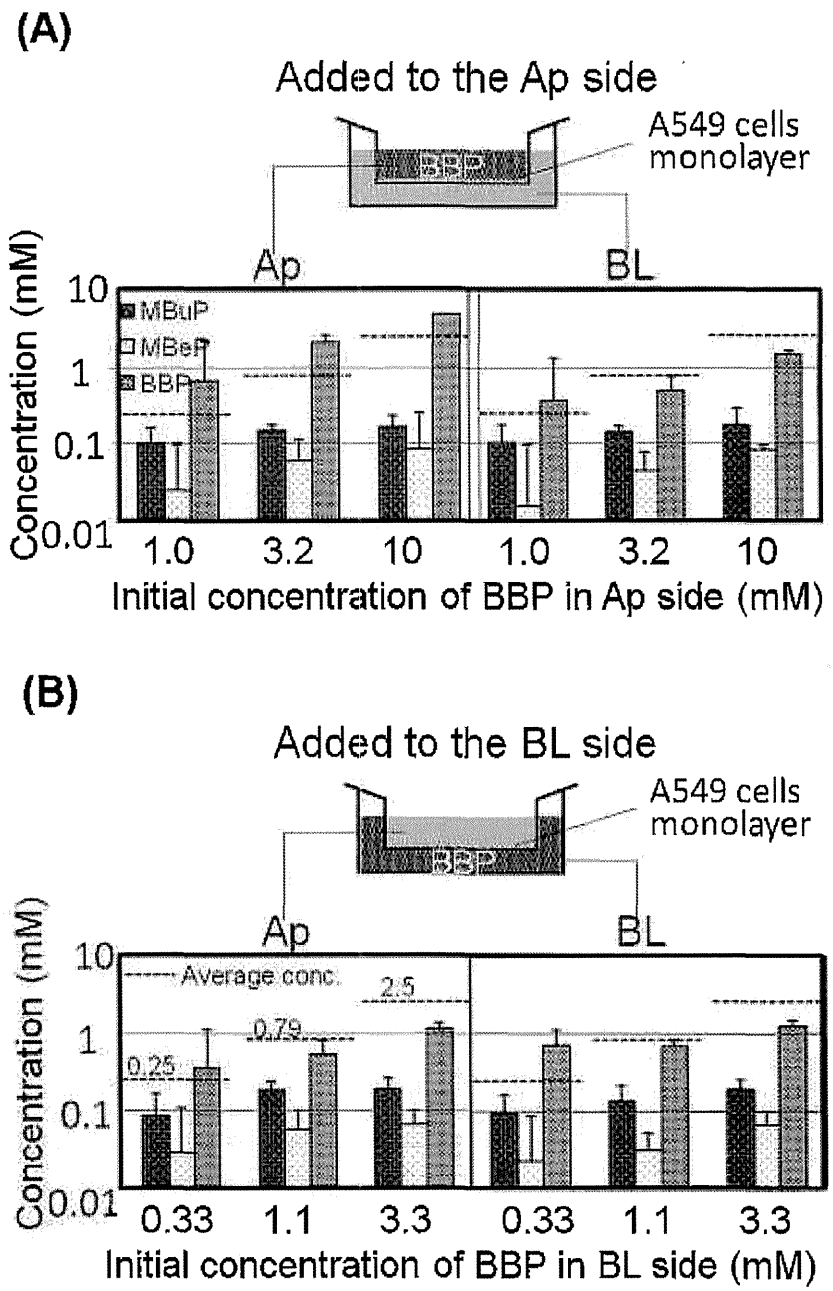

Figure 4 The amounts of monobutyl phthalate (MBuP), monobenzyl phthalate (MBeP), and benzylbutyl phthalate (BBP) on the apical (Ap) and basolateral (BL) sides 48 h after adding BBP to the Ap (A) or BL (B) side. BBP was metabolized to MBuP and MBeP, and a portion of the metabolites permeated through the cells.

Based on the aforementioned results, the following three points were considered in the analysis of long-term exposure of BBP in the mathematical model:

1 BBP is toxic to cells at concentrations exceeding 0.1 mM.
2 The effects of MBuP and MBeP are negligible.
3 The concentration of BBP on the Ap side (pulmonary alveolus side) is 3–4-fold higher than that on the BL side (blood) 48 h after loading BBP on the Ap side, whereas the BBP concentrations were nearly identical on both sides when BBP was initially added to the BL side.

Therefore, the transport of BBP from the Ap side to the BL side (from alveoli to blood) is considered very slow compared with that in the opposite direction. Conversely, BBP antiport may be occurring.

In consideration of these points, the numerical model comprising three compartments, the Ap side (inner space of the pulmonary alveolus), cell layer (alveolus epithelium), and BL side (pulmonary blood circulation) compartments, was developed by assuming dynamic equilibrium among the three compartments. BBP is transferred by the following four processes:

i. Transport from the Ap side to the cells
ii. Transport from the cells to the Ap side
iii. Transport from the cells to the BL side
iv. Transport from the BL side to the cells

Figure 5 shows these processes, compartments, and the material balances in each compartment. From the Ap side to the cell layer (i), BBP transport occurred through the lipid bilayer of the cell membrane, and the rate of transfer depended on the BBP concentration. The transfer rate is proportional to the transfer coefficient; therefore, the transportation in this process is represented by the following formula:

$$J = -k_1 \cdot \mathrm{A} \cdot C_{Ap}$$

where k_1 is the mass-transfer coefficient of (i), A is the area of transfer, and C_1 is the concentration on the Ap side. The transfer rate of BBP from the cell layer to the Ap side (ii) is proportional to the transfer coefficient. Thus, transportation in this process is represented by the following formula:

$$J = -k_2 \cdot \mathrm{A} \cdot C_{CL}$$

where k_2 is the mass-transfer coefficient of (ii) and C_{CL} is the concentration in the cell layer. Transportation in process (iii), which was the same as that in process (i), is represented by the following formula:

$$J = -k_3 \cdot \mathrm{A} \cdot C_{CL}$$

where k_3 is the mass-transfer coefficient of (iii), and transportation via this process is represented by the following formula:

$$J = -k_4 \cdot \mathrm{A} \cdot C_{BL}$$

where k_4 is the mass-transfer coefficient of (iv) and C_{BL} is the concentration on the BL side.

To determine these parameters (k_1 – k_4), and A549 cells were cultured on the membrane

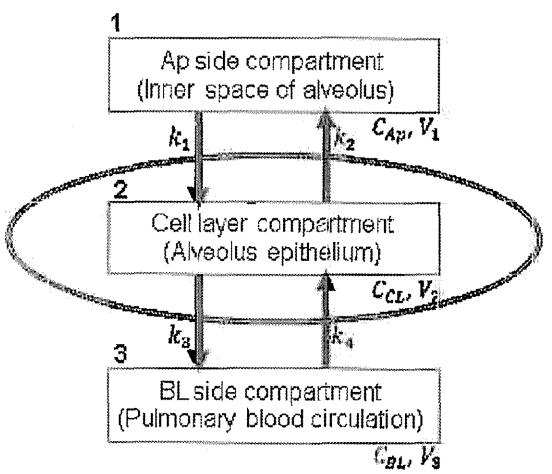

1. $V_1 \cdot dC_{Ap}/dt = (-k_1 \cdot C_{Ap} + k_2 \cdot C_{CL}) \cdot A$
2. $V_2 \cdot dC_{CL}/dt = (k_1 \cdot C_{Ap} - (k_2 + k_3) \cdot C_{CL} + k_4 \cdot C_{BL}) \cdot A$
3. $V_3 \cdot dC_{BL}/dt = (k_3 \cdot C_{CL} - k_4 \cdot C_{BL}) \cdot A$

C_i : concentration in the compartment i
V_i : volume of the compartment i
k_i : mass-transfer coefficient

Figure 5 The numerical model composed of three compartments: apical side (inner space of the alveolus), cell layer (alveolus epithelium), and basolateral side compartments (pulmonary blood circulation). BBP is transferred by four processes, and the three equations represent the material balances in each compartment.

in the culture insert and BBP-containing medium was added onto the A549 monolayer. In both experiments, the changes of the BBP concentration were measured for 48 h. The results for these experiments are shown as solid circles in Fig. 6 (a) and (b), respectively.

In the system in which monolayer cells were cultured in a tissue culture dish, there are only two compartments, the Ap side (inner space of alveolus) and cell layer compartments (alveolus epithelium), and the material transfer equations for each compartment are as follows:

$$\text{Ap side: } V_1 \cdot dC_{AP}/dt = (-k_1 \cdot C_{AP} + k_2 \cdot C_{CL}) \cdot A \quad (1)$$

$$\text{Cell layer: } V_2 \cdot dC_{CL}/dt = (-k_1 \cdot C_{AP} + k_2 \cdot C_{CL}) \cdot A \quad (2)$$

In this system, the thickness of the A549 cell layer was assumed to be 10 μm, and the cell layer volume V_{CL} is 7.9×10^{-2} cm^3 because a 10-cm dish was used for this experiment. As C_2 was almost zero soon after BBP exposure, the equation becomes

$$V_1 \cdot dC_{AP}/dt = -k_1 \cdot C_{AP} \cdot A \quad (3)$$

where A = 79 cm^2 and V_1 = 10 cm^2. As at $T_{ex} = 0$ is calculated from the slope of the curve, it is determined to be $k_1 = 2.5 \times 10^{-2}$ cm/h at the initial BBP concentration. The slope was determined by least squared approximation with 2, 3 data around $T = 0$. Conversely, when equilibrium is attained, the mass balance in each compartment is stable, and the equation becomes

$$k_1 \cdot C_{AP} - k_2 \cdot C_{CL} = 0 \quad (4)$$

k_2 is calculated as 1.6×10^{-4} cm/h using equation (4), the total mass balance, and a saturated concentration of BBP. This saturated concentration was determined by averaging the concentrations of T = 24, 46 h.

The system in which cells are cultured in

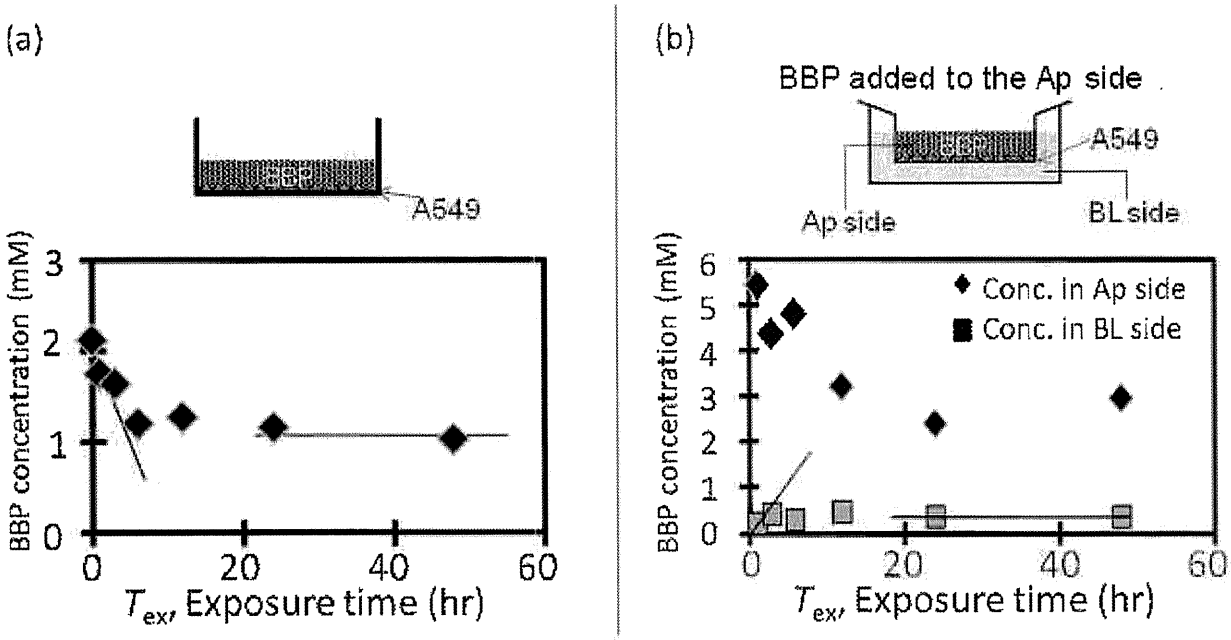

Figure 6 The time-dependent changes of the BBP concentration when cells cultured in a monolayer in a tissue culture dish (a) or on the membrane of a culture insert (b) were exposed to BBP.
The parameters (k_1-k_4) were calculated at $T_{ex} = 0$ and the equilibrium BBP concentration.

the culture insert includes all three compartments as shown in Fig. 5. The parameters (k_3 and k_4) were calculated to be 8.4×10^{-4} and 0.67 cm/h, respectively, as described previously. The calculated parameters are summarized in Table 1. With the parameters ($k_1 - k_4$) and equations (1) and (2), the time-dependent concentrations of BBP were calculated and presented as lines in Fig. 7. The calculated data were consistent with the measured data, and the correlation coefficients are 0.84 for Apical side and 0.67 for Basolateral side. It was found that the values of k_1 and k_4 were substantially higher than those of k_2 and k_3 because 10 μmol BBP at the measured value was predicted to be transported and exist in the cells in a small volume of 7.8×10^{-2} cm^3 and the BBP concentration inside the cells is extremely high; and this high concentration causes the low coefficient value of k_2 and k_3.

Prediction of in vivo BBP permeation using the simulation

The in vivo level of BBP exposure was mimicked in this study, although there were two differences between our system and the actual in vivo situation. (1) The total surface area of alveoli was reported to be 30–50 m^2, which was 4.0 $\times$ 10^5-fold greater than that in the present experiment. In addition, the thickness of alveoli was 0.5 μm compared with a thickness of approximately 10 μm in the present study (Kierszenbaum, 2007). (2) The BL side was as-

Table 1 The calculated values of parameters (k_1-k_4) with the time-dependent changes of the BBP concentration when the cells were exposed to BBP.

Parameter		
k_1	Mass transfer coefficient from Ap side to cells	2.5×10^{-2}
k_2	Mass transfer coefficient from cells to Ap side	1.6×10^{-4}
k_3	Mass transfer coefficient from cells to BL side	8.4×10^{-4}
k_4	Mass transfer coefficient from BL side to cells	6.7×10^{-1}

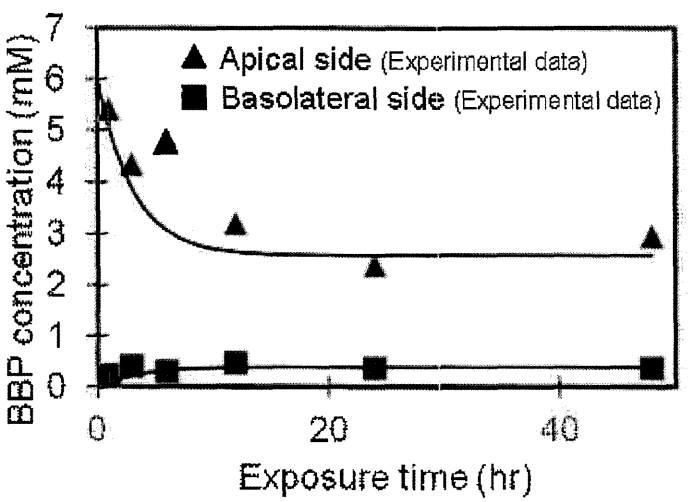

Figure 7 The time-dependent concentrations of BBP calculated using parameters (k_1-k_4) and equations (1) and (2) (shown as lines).
The calculated data are consistent with the measured data.

sumed to represent the blood, but blood is constantly perfused in the actual in vivo environment. Moreover, the perfusion rate is high, and the concentration of phthalate in blood is assumed to be zero (Ramsey *et al.*, 1984). We therefore changed the parameters concerning these points to improve the correspondence of the model to the in vivo situation.

The time-dependent amount of BBP accumulated in epithelial cells when 6,1μM BBP was initially added to the cells is indicated in Fig. 8 (a), and the total amount of BBP that permeated through the cells is shown in Fig. 8 (b). The total amount of BBP in epithelial cells increased for 1.5 h and equilibrated at 0.30 μmol/cm^2, and the total amount of BBP permeated into the blood reached 0.13 μmol/cm^2.

First, we changed the thickness of the alveolus epithelial cell layer from 10 to 0.5 μm and calculated the total amounts of accumulated and permeated BBP as shown in the second column of Fig. 8. The total amount of accumulated BBP in cells drastically decreased compared with that at a cell thickness of 10 μm; conversely, the total amount of BBP that permeated through the cells was 0.24 μmol/cm^2, which was higher than that observed with a cell thickness of 10 μm.

In addition to changing the thickness of the cell layer, we assumed that the concentration on the BL side (i.e., the concentration of blood) was set at zero, and the calculated graphs are shown in the third column of Fig. 8. Under this condition, the BBP accumulation curve is different from the other two curves. The total amount of BBP accumulated drastically changed to 6.9 × 10^{-3} μmol/cm^2 and then gradually decreased to zero over approximately 24 h, and the total amount of BBP that permeated through the cells was 0.76 μmol/cm^2.

The simulation revealed that even if the in vitro cell-based tissue model does not perfectly

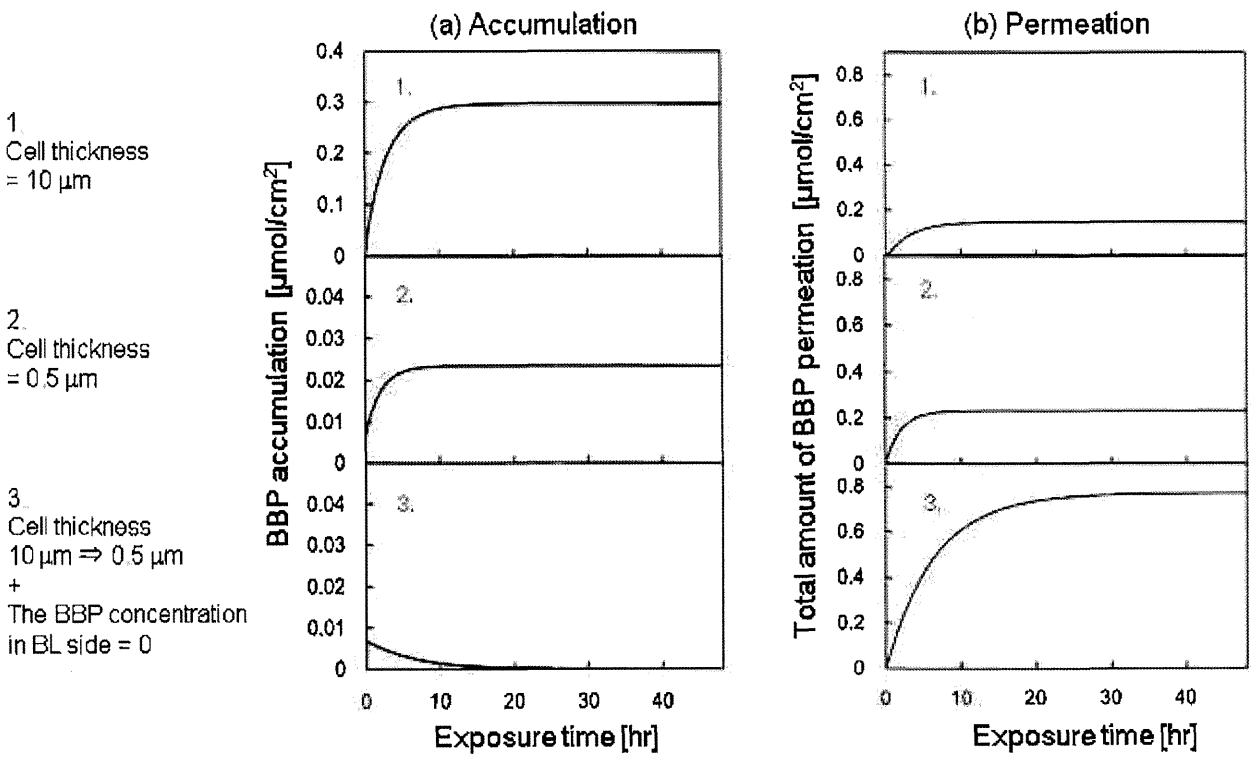

Figure 8 The time-dependent accumulation of BBP by epithelial cells (a) and the total amount of BBP permeated through the cells (b) when 6.1μM BBP was added to the apical (Ap) side.
The time-dependent curve calculated after changing the thickness of the cell layer from 10 (A549 cells) to 0.5μm (alveoli) is shown in the second column, and that when the basolateral concentration was assumed to always be zero is shown in the third column.

mimic the in vivo situation with regard to some parameters, we could overcome the limitations and/or properties of the culture models by using numerical simulations to change various parameters and assumptions in a scientifically rational manner. To predict hazards in a better manner in humans, it is important to establish an animal-free cell based model with an understanding of the parameters that differ from the in vivo condition and adjust them as needed in the numerical simulation.

From the results of the simulations, it was found that BBP inhaled into the alveoli is transported to the blood through the pulmonary epithelium for approximately 24 h in vivo as opposed to remaining in the cells. The accumulation of BBP by cells can cause epithelial damage, but the amount of BBP accumulated by cells is always less than 6.9×10^{-3} μmol/cm^2 and decreases to zero within 24 h. Therefore, these results suggest that the possibility of epithelial damage in vivo is low after BBP inhalation and these experiments using A549 cell monolayers in culture dishes could overestimate the possibility of cellular damage.

BBP, which permeates through cells to the blood, reaches other organs via the bloodstream. Previous in vivo experiments revealed that phthalate targets germ cells in the testis (David *et al.*, 2000; Lamb *et al.*, 1987). These data are consistent with the results of this study that BBP passes through cells to the bloodstream, could not be metabolized or eliminated by organs such as the liver and kidneys, and is ultimately expected to be transported to these organs (Jian, 2012). This study demonstrated that estimating the perfusion of target chemicals in the blood flow is important.

One point that should be mentioned is that the adsorption of BBP to plastics is not considered in our model. Phthalates have relatively high affinity for the surfaces of experimental instruments such as dishes and flasks, especially those made of plastic (Thomsen *et al.*, 2001). In the experiments in this study, we noticed that small amounts of BBP were lost during the procedures. These small amounts were disregarded in this study, which may result in overestimation of the amount of BBP transported to the cells. However, investigating the adsorption of BBP could be a single comprehensive subject of research because many types of plastics are used as culture apparatus and the adsorption of BBP is different for each type. In addition, adsorption is affected by conditions such as temperature, pressure, time, and the dispersion medium. Therefore, we would like to investigate this subject in a future project.

Conclusion

We identified problems in the integrated uses of permeation data for BBP in an A549 cell-based culture model using a culture insert and created a simple numerical simulation to determine the toxicity of substances in humans. The model described high accumulation of BBP in the alveolus cell layer (0.30 μmol/cm^2) at equilibrium, and therefore, we changed the thickness of the cell layer from 10 (A549 cells) to 0.5 μm (alveoli) and also incorporated the assumption that the BL concentration is always zero because the perfusion of blood in vivo. Further, the amount of accumulated BBP decreased over approximately 24 h, and the maximum amount of accumulated BBP was 6.9×10^{-3} μmol/cm^2. Moreover, the total amount of permeated BBP increased from 0.13 to 0.76 μmol/cm^2 after adjusting the aforementioned parameters. These results indicate that when in vitro cell-based tissue models and numerical simulations are used to predict toxicity in humans in an animal-free environment, various parameters and assumptions should be changed in a scientifically rational manner to overcome the limitations and/or properties of existing culture models to improve the predictive accuracy of the system.

References

Alink, G. M., de Boer, R. M., Mol, J., and Temmink, J. H. (1980) Toxic effects of ozone on human cells in vitro, exposed by gas diffusion through teflon film, Toxicology, **17**, 209–218.

Autian, J. (1973) Toxicity and health threats of phthalate esters: review of the literature, Environ Health Perspect, **4**, 3–26.

Banks, M. A., Porter, D. W., Martin, W. G., and Castranova, V. (1990) Effects of in vitro ozone exposure on peroxidative damage, membrane leakage, and taurine content of rat alveolar macrophages, Toxicol Appl Pharmacol, **105**, 55–65.

Bolton, D. C., Tarkington, B. K., Zee, Y. C., and Osebold, J. W. (1982) An in vitro system for studying the effects of ozone on mammalian cell cultures and viruses, Environ Res, **27**, 466–475.

Bornehag, C.-G., Lundgren, B., Weschler, C. J., Sigsgaard, T., Hagerhed-Engman, L., and Sundell, J. (2005) Phthalates in indoor dust and their association with building characteristics, Environ Health Perspect, 113, 1399–1404.

Cheek, J. M., Postlethwait, E. M., and Crandall, E. D. (1988) Effects of culture conditions on susceptibility of alveolar epithelial cell monolayers to NO2, Toxicol Lett, **40**, 247–255.

David, R., Moore, M., Finney, D., and Guest, D. (2000) Chronic toxicity of di(2-ethylhexyl)phthalate in rats, Toxicol Sci, **55**, 433–443.

Dumler, K., Hanley, Q. S., Baker, C., Luchtel, D. L., Altman, L. C., and Koenig, J. Q. (1994) The effects of ozone exposure on lactate dehydrogenase release from human and primate respiratory epithelial cells, Toxicol lett, **70**, 203–209.

Ema, M., Miyawaki, E., and Kawashima, K. (2000) Effects of dibutyl phthalate on reproductive function in pregnant and pseudopregnant rats. Reproductive toxicology (Elmsford, N.Y.), 14, 13–19.

European Chemicals Bureau (2007) Benzyl butyl phthalate (BBP) European Union risk assessment report. http://ecb.jrc.it/DOCUMENTS/ Existing-Chemicals/RISK_ASSESSMENT/ REPORT/ benzylbutylphthalatereport 318.pdf.

Giam, C. S., Chan, H. S., Neff, G. S., and Atlas, E. L. (1978) Phthalate ester plasticizers: a new class of marine pollutant. Science (New York, N.Y.), 199, 419–421.

Guerrero, R. R., Rounds, D. E., Booher, J., Olson, R. S., and Hackney, J. D. (1979) Ozone sensitivity in aging WI-38 cells based on acid phosphatase content, Arch Environ Health, **34**, 407–412.

Hosokawa, M. and Satoh, T. (2002) Measurement of carboxylesterase (CES) activities. Current protocols in toxicology / editorial board, Mahin D. Maines (editor-in-chief) ... [et al.], Chapter 4, Unit4.7.

IARC (2000) monographs on the evaluation of carcinogenic risks to humans. some industrial chemicals - Google 検索. International Agency for Research on Cancer, Lyon, France, pp.77.

Jian Ge (2012) Study on metabolism of N-Butyl Benzyl Phthalate (BBP) and Dibutyl Phthalate (DBP) in Ctenopharyngodon idellus by GC and LC-MS/MS. African Journal of Agricultural Research, 7(12). [online] http://www. academicjournals.org/ajar/abstracts/abstracts/abstract 2012/ 26%20Mar/ Ge%20%20et%20al.htm (Accessed December 18, 2012).

Kierszenbaum, A. (2007) Histology and Cell Biology: An Introduction to Pathology. Second Edition. Mosby . Elsevier Health Sciences, 388.

Konings, A. W. (1986) Mechanisms of ozone toxicity in cultured cells. I. Reduced clonogenic ability of polyunsaturated fatty acid-supplemented fibroblasts. Effect of vitamin E. J Toxicol Environ Health, **18**, 491–497.

Lamb, J. C., 4th, Chapin, R. E., Teague, J., Lawton, A. D., and Reel, J. R. (1987) Reproductive effects of four phthalic acid esters in the mouse, Toxicol Appl Pharmacol. **88**, 255–269.

Martin, A. and Clynes, M. (1993) Comparison of 5 microplate colorimetric assays for in vitro cytotoxicity testing and cell proliferation assays. Cytotechnol, **11**, 49–58.

Van Meeuwen, J. A., Ter Burg, W., Piersma, A. H., van den Berg, M., and Sanderson, J. T. (2007) Mixture effects of estrogenic compounds on proliferation and pS2 expression of MCF-7 human breast cancer cells, Food Chem Toxicol, **45**, 2319-2330.

Nativelle, C., Picard, K., Valentin, I., Lhuguenot, J. C., and Chagnon, M. C. (1999) Metabolism of n-butyl benzyl phthalate in the female Wistar rat. Identification of new metabolites, Food Chem Toxicol, **37**, 905–917.

Nikula, K. J. and Wilson, D. W. (1990) Response of rat tracheal epithelium to ozone and oxygen exposure in vitro, Fundam Appl Toxicol, **15**, 121-131.

Pace, D. M., Landolt, P. A., and Aftonomos, B. T. (1969) Effects of ozone on cells in vitro, Arch Environ Health, **18**, 165–170.

Pan, G., Hanaoka, T., Yoshimura, M., Zhang, S., Wang, P., Tsukino, H., Inoue, K., Nakazawa, H., Tsugane, S., and Takahashi, K. (2006) Decreased serum free testosterone in workers exposed to high levels of di-n-butyl phthalate (DBP) and di-2-ethylhexyl phthalate (DEHP): a cross-sectional study in China, Environ Health Perspect, **114**, 1643–1648.

Patel, J. M., Sekharam, K. M., and Block, E. R. (1990) Oxidant injury increases cell surface receptor binding of angiotensin II to pulmonary artery endothelial cells, J Biochem Toxicol, **5**, 253–258.

Peakall, D. B. (1975) Phthalate esters: Occurrence and biological effects, Residue Rev, **54**, 1–41.

Ramsey, J. C. and Andersen, M. E. (1984) A physiologically based description of the inhalation pharmacokinetics of styrene in rats and humans, Toxicol Appl Pharmacol, 73, 159-175.

A physiologically based description of the inhalation pharmacokinetics of styrene in rats and humans, Toxicol Appl Pharmacol, **73**, 159–175.

Ross, M. K., Borazjani, A., Wang, R., Crow, J. A., and Xie, S. (2012) Examination of the carboxylesterase phenotype in human liver, Arch Biochem Biophys, **522**, 44–56.

Salazar, V., Castillo, C., Ariznavarreta, C., Campón, R., and Tresguerres, J. A. F. (2004) Effect of oral intake of dibutyl phthalate on reproductive parameters of Long Evans rats and pre-pubertal development of their offspring, Toxicol, **205**, 131–137.

Thomsen, M., Carlsen, L., and Hvidt, S. (2001) Solubilities and surface activities of phthalates investigated by surface tension measurements, Environ Toxicol Chem, **20**, 127–132.

Vesterkvist, P. S. M., Misiorek, J. O., Spoof, L. E. M., Toivola, D. M., and Meriluoto, J. A. O. (2012) Comparative cellular toxicity of hydrophilic and hydrophobic microcystins on caco-2 cells, Toxins, **4**, 1008–1023.

Wormuth, M., Scheringer, M., Vollenweider, M., and Hungerbühler, K. (2006) What are the sources of exposure to eight frequently used phthalic acid esters in Europeans? , Risk Anal, **26**, 803–824.

Yang, T. T., Sinai, P., and Kain, S. R. (1996) An acid phosphatase assay for quantifying the growth of adherent and nonadherent cells, Anal Biochem, **241**, 103–108.

(Received: April 23, 2013/
Accepted: September 24,2013)

Corresponding author:
Kokoro IWASAWA, Ph., D.
Institute of Industrial Science,
the University of Tokyo
Department of Materials and
Environmental Science
Sakai Lab.
4-6-1 Komaba, Meguro-ku, Tokyo,
153-8505 JAPAN
Tel: +81-3-5452-6349
Fax: +81-3-5452-6353
E-mail: kokoro@iis.u-tokyo.ac.jp

Chemosphere 102 (2014) 24–30

Contents lists available at ScienceDirect

Chemosphere

journal homepage: www.elsevier.com/locate/chemosphere

Simple and rapid determination of PCDD/Fs in flue gases from various waste incinerators in China using DR-EcoScreen cells

Zhiguang Zhou [a,b,*], Bin Zhao [a], Hiroyuki Kojima [c], Shinji Takeuchi [c], Yoko Takagi [d], Norio Tateishi [d], Mitsuru Iida [e], Takuya Shiozaki [f], Pengjun Xu [b], Li Qi [b], Yue Ren [b], Nan Li [b], Sen Zheng [b], Hu Zhao [b], Shuang Fan [b], Ting Zhang [b], Aimin Liu [b], Yeru Huang [b]

[a] State Key Laboratory of Environmental Chemistry and Ecotoxicology, Research Center for Eco-Environmental Sciences, Chinese Academy of Sciences, Beijing 100085, China
[b] State Environmental Protection Key Laboratory of Dioxin Pollution Control, National Research Center for Environmental Analysis and Measurement, 1 South Yuhui Rd, Chaoyang District, Beijing 100029, China
[c] Hokkaido Institute of Public Health, Kita-19, Nishi-12, Kita-ku, Sapporo 060-0819, Japan
[d] Kyoto Electronics Company, Ltd., 68 Ninodan-cho, Shinden, Kisshoin, Minami-Ku, Kyoto 601-8317, Japan
[e] Diagnostic Division, Otsuka Pharmaceutical Company, Ltd., Tokushima 771-0195, Japan
[f] Japan Environment Sanitation Center, 1182 Sowa, Nishi-ku, Niigata 950-2144, Japan

HIGHLIGHTS

- We construct an automated sample preparation device (SPD-600) for bioassay.
- We construct a new, sensitive and rapid reporter gene system for PCDD/Fs.
- Utilizing SPD-600 coupled cell to determine four different flue gases in China.
- Utilizing SPD-600 coupled cell can be a useful and prescreening method in China.

ARTICLE INFO

Article history:
Received 9 May 2013
Received in revised form 21 October 2013
Accepted 1 December 2013
Available online 28 December 2013

Keywords:
Aryl hydrocarbon receptor
Flue gas
Reporter gene assay
PCDD/Fs

ABSTRACT

In developing countries such as China, there is a strong need for simple and rapid bioassays for the determination of polychlorinated dibenzo-p-dioxins and dibenzofurans (PCDD/Fs) in environmental samples; i.e., flue gas and fly ash from waste incinerators. In this study, we applied the DR-EcoScreen cell (DR-cell) assay to determination of PCDD/Fs in 78 flue gas samples obtained from various waste incinerators in China between 2009 and 2011. The flue gas samples were obtained from four kinds of incinerators, classified into hazardous, medical and municipal-solid waste, and iron ore sintering, and the flue gas extracts were cleaned up using an SPD-600 automated-sample preparation device for DR-cell assay. The PCDD/Fs values obtained from the DR-cell assay were compared with those obtained from conventional high resolution gas chromatography–high resolution mass spectrometry (HRGC–HRMS) analysis. The bioanalytical equivalent (BEQ) values obtained from the DR-cell assay were very closely correlated with the international toxicity equivalent (I-TEQ) values from HRGC–HRMS analysis ($r^2 = 0.98$, $n = 78$), while the BEQ values were 5.52-fold higher than the I-TEQ values, as the PCDFs, which account for 80% of the total I-TEQ value, were overestimated by DR cell-assay. Therefore, we multiplied the BEQ values from the DR-cell assay by a conversion coefficient (0.181, the reciprocal of 5.52), and could approximate the TEQ values from the HRGC–HRMS analysis. These results suggest that the DR-cell assay combined with SPD-600 cleanup provides a promising method for the simple and rapid screening of PCDD/Fs levels in flue gas samples, such as those from various waste incinerators in China.

© 2013 Elsevier Ltd. All rights reserved.

1. Introduction

China is facing growing environmental pressure due to the rapid economic development and urbanization occurring over the last three decades. Consequently, the quantity of various wastes has increased at a high rate, and their disposal has had a great impact on the environment and on public health. To dispose of

* Corresponding author at: State Key Laboratory of Environmental Chemistry and Ecotoxicology, Research Center for Eco-Environmental Sciences, Chinese Academy of Sciences, Beijing 100085, China. Tel.: +86 10 84665758; fax: +86 10 84634275.
E-mail address: zzguang2004@hotmail.com (Z. Zhou).

0045-6535/$ - see front matter © 2013 Elsevier Ltd. All rights reserved.
http://dx.doi.org/10.1016/j.chemosphere.2013.12.006

huge amounts of solid waste at low-cost and in an environmentally friendly manner, many incinerators have been constructed in China. Although incineration offers many advantages, such as significant volume and mass reduction, some secondary pollution with the release of compounds, such as heavy metals (Jung et al., 2004; Yao et al., 2012), polychlorinated dibenzo-p-dioxins (PCDDs) and polychlorinated dibenzofurans (PCDFs) (Shibamoto et al., 2007; Ni et al., 2009).

These PCDD/Fs, so-called dioxins, are produced as unintentional by-products, and enter the environment via incineration, thermal processes and chemical manufacture (Zheng et al., 2008). These PCDD/Fs are widely distributed contaminants that are persistent and bio-accumulative, and can induce various toxic responses including immunotoxicity, carcinogenicity, as well as having adverse effects on reproduction, development, and endocrine functions via aryl hydrocarbon receptor (AhR) (Poland and Knutson, 1982; Safe, 1986; Fernandez-Salguero et al., 1996; Mimura et al., 1997). Therefore, the Chinese government has imposed standarzdized limits on PCDD/F emissions from flue gas of 1.0 ng I-TEQ N m^{-3} for municipal solid waste incinerators and 0.5 ng I-TEQ N m^{-3} for medical and hazardous waste incinerators. A better understanding of the levels and distribution of these compounds will allow more appropriate measures to be employed to reduce their emission.

The "gold standard" chromatographic technique based on high resolution gas chromatography–high resolution mass spectrometry (HRGC–HRMS) has been extensively used for the conventional determination of 17 PCDD/Fs (Firestone, 1991; Jong et al., 1993; Singh and Kulshrestha, 1997). The measured values of 17 PCDD/Fs are individually multiplied by a toxicity equivalency factor (TEF) and totaled to give I-TEQ values (Van den Berg et al., 2006). This method provides reliable data including the concentration of each of the 17 congeners in the test samples. However, it also requires expensive equipment and highly trained analysts, whilst the sample preparation procedures are time-consuming and costly. In particular, this method might be less than useful when rapid data on PCDD/Fs from a large set of test samples is required. For this reason, the development of a rapid and inexpensive screening method for PCDD/Fs remains a high priority, especially in developing countries with limited resources, such as China. Thus, there is a definite need to develop a faster and lower-cost bioassay methods for the determination of PCDD/Fs.

Reporter gene assays using hepatocarcinoma cells, which express the AhR gene and luciferase reporter gene containing the dioxin-responsive element (DRE), are applicable to the detection of dioxin-like compounds based on their activation of AhR (Garrison et al., 1996; Murk et al., 1996). Recently, Takeuchi have developed a new, sensitive and rapid reporter gene assay (DR-cell assay) using a genetically engineered stable cell line, designated DR-EcoScreen cells. The minimal detection limit (MDL) and 50% effective concentration (EC_{50}) of 2,3,7,8-TetraCDD (TCDD) in this DR-cell assay are 0.1 pM and 2.8 pM, respectively, with little variance observed in the data (within CV 10%), but other reporter gene assays, such as, Hepa1c1c7- and H4IIE-based CALUX assays, the MDL of 2,3,7,8-TCDD were reported to be 1 and 0.3 pM, and the EC_{50} of 2,3,7,8-TCDD were reported to be 10 and 10 pM, respectively (Behnisch et al., 2002; Han et al., 2004). Besides high sensitivity, the DR-cell assay has unique advantages compared to other bioassays. As the DR-EcoScreen cells have very strong luminescence intensity and can be measured using a long-lived luciferase substrate, a bioassay using these cells does not require well-washing or medium changes during the procedure. Thus, the DR-cell assay is compatible with high-throughput automation and can reduce the overall workload in a laboratory. Most recently, based on a comparative study with HRGC–HRMS analysis, it has been reported that the DR-cell assay was helpful in determining low levels of PCDD/Fs and dioxin-like polychlorinated biphenyls (PCBs) in ambient air samples (Anezaki et al., 2009) as well as in fish and seafood samples (Kojima et al., 2011).

In the present study, we investigated the applicability of the DR-cell assay to the determination of PCDD/Fs in 78 flue gas samples from four kinds of incinerators, including medical waste and municipal solid waste incinerators, in China as a prescreening step to the HRGC–HRMS method. In addition, we have now combined the DR-cell assay with a cleanup procedure utilizing an SPD-600 automated-sample preparation device. The bioanalytical equivalent (BEQ) values from the DR-cell assay were compared with the I-TEQ values from the HRGC–HRMS analysis, and we found that the values from both methods showed a very close correlation. Here, we provide evidence that the DR-cell assay coupled with SPD-600 cleanup might afford a promising method for the simple and rapid screening of PCDD/Fs in flue gas, such as that from various waste incinerators in China.

2. Materials and methods

2.1. Chemicals and cell culture materials

Acetone, *n*-hexane, toluene, and dichloromethane were obtained from J.T. Baker, Co., Ltd. (USA). Dimethyl sulfoxide (DMSO) and some kinds of silica gel for multi-layer column chromatography were obtained from Wako Pure Chemicals Inc., Ltd. (Osaka, Japan). The PCDD/F standards were obtained from Wellington Laboratories (Canada).

Fetal bovine serum (FBS), alpha-modified Eagle's minimum essential medium (α-MEM) and hygromycin were obtained from Invitrogen (San Diego, CA, USA). Glutamine and penicillin–streptomycin (antibiotics) solutions were obtained from Dainippon Pharmaceutical Co., Ltd. (Osaka, Japan). A 0.25% trypsin/0.02% ethylenediamine tetra-acetic acid (EDTA) disodium salt solution was obtained from Life Technologies (Paisley, UK). The luciferase substrate, Steady-Glo™ reagent, was purchased from Promega (Madison, WI, USA).

2.2. Collection, extraction, and cleanup of flue gas samples

We collected 19, 20, 21, and 18 flue gas samples from hazardous waste incinerators (i.e., chemical plants, and pesticide and paint factories), medical waste incinerators, municipal solid waste incinerators, and iron ore sintering furnaces, respectively, in China between 2009 and 2011. PCDD/Fs in flue gas were captured by a quartz filter cylinder, and XAD-2 resin with a vacuum pump (TCR TECORA, Italy) (gas volume approximately 3 m^3, 0 °C and 1 atm). Each sample was then extracted with 300 mL of toluene by soxhlet for 24 h. The solvent was reduced to around 1 mL in a rotary evaporator, then 100 mL *n*-hexane was added. The *n*-hexane solution was treated with 20 mL of concentrated sulfuric acid until the *n*-hexane layer became colorless. After washing the extract twice with 50 mL of 2% NaCl solution, it was evaporated to a 1 mL in a rotary evaporator.

As shown in Fig. 1a, the cleanup of samples was conducted using two different methods: cleanup for the DR-cell assays employed an SPD-600 automated-sample preparation device (Kyoto Electronics Company, Ltd., Kyoto, Japan), whereas the cleanup for the HRGC–HRMS analysis used conventional manual chromatography columns, including a multi-silica gel column, an alumina column and a florisil column (JIS K0311, 1999). The SPD-600 device has a multilayer silica gel column (12.5 × 200 mm) and an alumina column (0.8 g). The multilayer column is composed, from bottom up, of silica gel (0.5 g), 10% $AgNO_3$ silica gel, 44% H_2SO_4 silica gel (10 g), and silica gel (0.5 g). The PCDD/Fs were adsorbed on the

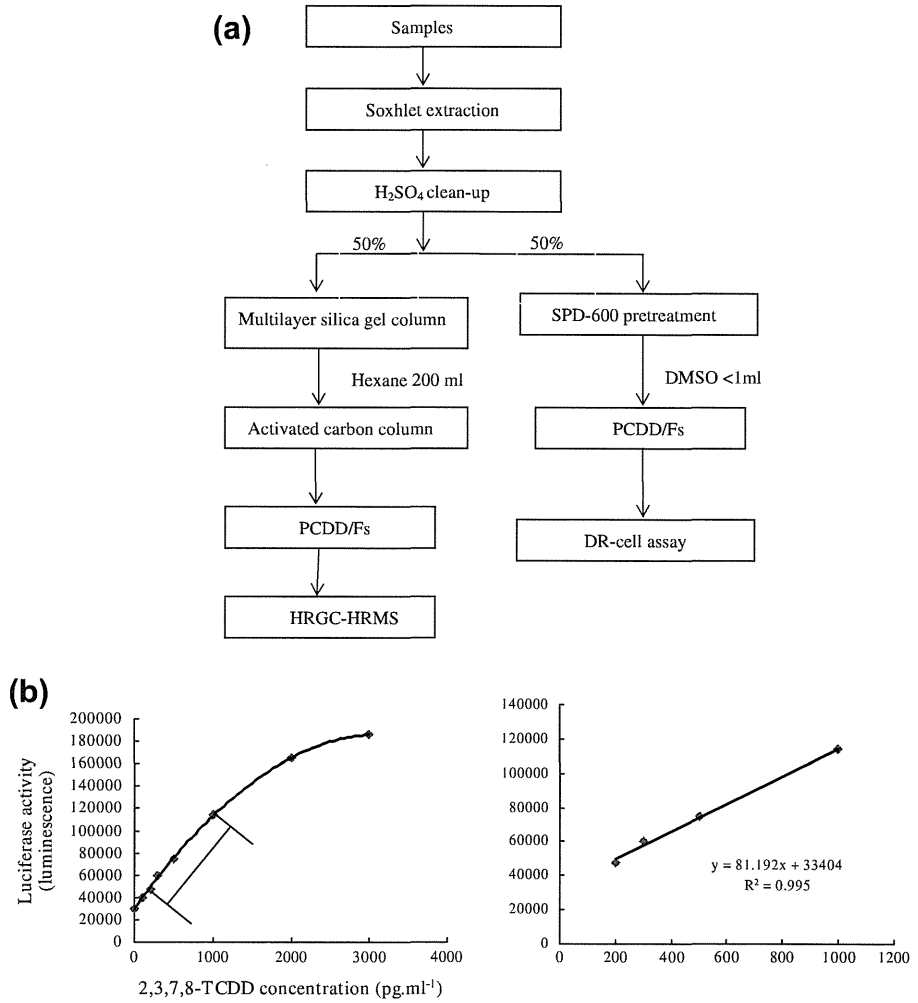

Fig. 1. Schema for the extraction and cleanup of flue gas samples for the DR-EcoScreen cell assay (a), and the standard curve and quantitative regression line for 2,3,7,8-TCDD as determined using this assay (b).

alumina column, and eluted with 0.7 mL DMSO. In the conventional manual cleanup for HRGC–HRMS, the extract was concentrated again then transferred to a vial. The solvent remaining in the vial was then reduced to about 20 μL by a gentle stream of nitrogen. ^{13}C-labeled PCDD/F recovery standard mixture was spiked prior to HRGC–HRMS analysis.

2.3. DR-EcoScreen cell bioassay

A highly sensitive AhR-mediated reporter cell line, DR-EcoScreen cells, developed from a mouse hepatoma Hepa1c1c7 cell line, was stably transfected with a reporter plasmid containing seven copies of DRE fused to a luciferase gene (Takeuchi et al., 2008). The DR-EcoScreen cells were maintained in α-MEM supplemented with 5% FBS, antibiotics, glutamine, and 150 μg mL^{-1} of hygromycin at 37 °C in an atmosphere of 5% CO_2 and 95% air under saturating humidity, and passaged twice every week by trypsinization with 0.25% trypsin/0.02% EDTA. For the screening assay, cells were trypsinized and suspended at a density of 1.0×10^5 cells mL^{-1} in α-MEM containing 5% CD-FBS. Ninety μL of the cell suspension was seeded in each well of a 96-well flat-bottomed plate (#136102 Nunclon™, Nalge Nunc, Denmark) at a final density of 9000 cells $well^{-1}$. After cultivation for 24 h at 37 °C, 10 μL of each of the various flue gas samples dissolved in 10% DMSO was added to each well (final concentration of DMSO was 1%). Following cultivation for a further 24 h, 100 μL of Steady-Glo™ reagent was added to each well. The plate was then shaken at room temperature for five min, and the luminescence was measured with a microplate-reader (Wallac 1420 ARVO™ SX, Perkin-Elmer). The dioxin concentrations in the samples were calculated as cell-based BEQ values using the quantitative regression line of the standard curve for 2,3,7,8-TCDD (Fig. 1b).

The validation of extremely sensitive responses for PCDD/Fs measurement for this cell were done by repeatedly analyzing the calibration standards ($n \geqslant 5$). The lowest concentration of the coefficient of variation (CV) < 30% was defined as the limit of detection (LOD). The lowest concentration of CV < 20% was defined as the limit of quantification (LOQ). The LOD and LOQ values for the bioassay were 0.1 and 0.2 pg mL^{-1} medium respectively. The LOD and LOQ could also be calculated to be 0.005 and 0.01 pg BEQ m^{-3} for about 1 L exhaust gas, respectively. And the quantitative regression line was set from 0.2 pg to 1.0 pg 2,3,7,8-TCDD mL^{-1}.

2.4. Quality control setting for DR-cell bioassay

Validation of this methodology requires strict quality control criteria, specifically designed for the DR-cell bioassay and quite different from the ones used in chemical analyses.

The first quality control is designed to assess the quality of the plates. For that purpose, a standard TCDD solution (50 pg mL^{-1} DMSO) was analyzed for each plate. The concentration of this solution was chosen to be in the middle of the quantifiable. The

averages (μ) and RSDs (σ) of many test results provide an assessment of the measurement repeatability on the 96 wells plate. According to the Western Electric Handbook (Montgomery, 2001), the control limits were $\mu \pm 3\sigma$, and the warning limits were $\mu \pm 2\sigma$. When the standard solution was not within the warning limits, the DR-cell bioassay was re-checked. On the basis of these criteria, 85% of the plates were accepted.

Secondly, a quality control sample (Certified reference material) was assessed by six complete analytical runs including every step from the exposer and light detection. For the reproducibility, the same sample was analyzed in duplicate on 6 different days. The CV of the repeatability and reproducibility test were 5% and 8%, respectively. Those values were lower than 20%, and could be accepted.

Thirdly, Recoveries of PCDD/Fs by these methods have been previously validated (Kojima et al., 2011).Finally, for the results to be accepted, the RLU ratio between samples and DMSO blank must more than 1.5.

2.5. HRGC–HRMS analysis

The quantification of 17 PCDD/Fs was performed by HRGC–HRMS on a 6890N Series gas chromatograph (Agilent Technologies, USA) coupled to an AutoSpec Ultima NT high-resolution mass spectrometer (Waters, USA). The injector was operated in splitless mode and kept at 270 °C. A DB-5ms capillary column (60 m × 0.25 mm i.d., 0.25 μm film thickness; Supelco, USA) was used for separation of the PCDD/Fs congeners. The column oven temperature was programmed at 160 °C for 2 min, increased to 220 °C at a rate of 5 °C min^{-1}, maintained at that temperature for 16 min, then increased to 235 °C at a rate of 5 °C min^{-1}, again maintained at that temperature for 7 min, then finally increased to 330 °C at a rate of 5 °C min^{-1}. The ion source was operated at 220 °C, with an electron energy of 45 eV, and selective ion monitoring (SIM) mode was used at resolution of >10000. Instrument detection limits were determined as a signal-to-noise ratio of 3:1. The measurement values were multiplied by I-TEF (Van den Berg et al., 2006) and totaled to obtain the I-TEQ.

The limits of detection (LODs) of HRGC–HRMS were around 0.01 pg m^{-3} for Tetra- and Penta-CDDs/Fs, 0.001–0.003 pg m^{-3} for Hexa- and Hepta-CDDs/Fs, and 0.002–0.004 pg m^{-3} for Octa-CDD/F. When the value was lower than the LOQ, the actual concentration was calculated as one-half of the LOD.

3. Results and discussion

3.1. Recovery capability and repeatability of PCDD/F determination in combination with an SPD-600 automated-sample preparation device

The recovery capability and repeatability of the SPD-600 method were tested by replicate analysis (3 times), and compared with those from the manual method used in conventional HRGC–HRMS analysis. Reference samples spiked with an internal standard were purified and substituted with DMSO solutions using the SPD-600 device. Thereafter, the DMSO solutions were substituted with hexane by liquid–liquid extraction, then determined by HRGC–HRMS. Table 1 shows the recovery averages and relative standard deviations (RSDs) of 17 PCDD/F concentrations obtained using the SPD-600 method and manual method. The recoveries of the SPD-600 method ranged from 87% to 107% whereas those obtained using the manual method ranged from 78% to 122%, suggesting that scatter of the values from the SPD-600 method was smaller than that from the manual method. In addition, the RSDs obtained from SPD-600 method (2–8%) were also smaller than those from manual method (1–19%), indicating that the repeatability of SPD-600 method is superior to that of the manual method. These results indicate that the SPD-600 method may be a reliable and suitable for the PCDD/Fs cleanup procedure used in the DR-cell assay, and gives greatly improved efficiency.

Table 1
Comparison of recoveries between manual packed column method and alumina column on SPD-600.

Congeners	Manual method ($n = 3$)		SPD-600($n = 3$)	
	Recovery (%)	RSD (%)	Recovery (%)	RSD (%)
2,3,7,8-TeCDD	79	12	93	2
1,2,3,7,8-PeCDD	91	12	100	4
1,2,3,4,7,8-HxCDD	99	14	99	4
1,2,3,6,7,8-HxCDD	104	13	92	3
1,2,3,7,8,9-HxCDD	97	17	106	5
1,2,3,4,6,78-HpCDD	122	5	105	4
OCDD	122	2	102	8
2,3,7,8-TeCDF	78	15	92	2
1,2,3,7,8-PeCDF	90	13	103	2
2,3,4,7,8-PeCDF	88	13	90	2
1,2,3,4,7,8-HxCDF	93	15	104	2
1,2,3,6,7,8-HxCDF	100	15	97	3
1,2,3,7,8,9-HxCDF	91	19	87	4
2,3,4,6,7,8-HxCDF	99	13	98	3
1,2,3,4,6,7,8-HpCDF	121	6	102	2
1,2,3,4,7,8,9-HpCDF	113	7	107	3
OCDF	118	1	101	5

The automated pre-treatment system, consisting of a multi-layer silica gel column and an alumina column, employs two special techniques (heating multi-layer silica gel and automatic solvent substitution) that could remove interference from contaminants such as aromatic hydrocarbons, and allow concentration directly to a small volume of DMSO solution, and potentially reducing human error.

3.2. Comparison between DR-cell assay and HRGC–HRMS analysis of PCDD/Fs in flue gas samples from four type incinerators

DR-cell assay and HRGC–HRMS analysis were used to estimate PCDD/Fs levels in flue gas samples obtained from hazardous waste incineration ($n = 18$), medical waste incineration ($n = 20$), iron ore sintering ($n = 21$) and municipal solid waste incineration ($n = 19$) in China (the gas volume is based on 0 °C and 1 atm).

The PCDD/F concentrations in 18 flue gas samples from hazardous waste incinerators were determined, the BEQ and I-TEQ values obtained from DR-cell assay and HRGC–HRMS analysis were compared. We found that the I-TEQ values from the HRGC–HRMS analysis ranged from 0.02 to 0.62 ng I-TEQ N m^{-3}, whereas the BEQ values from the DR-cell assay ranged from 0.06 to 2.48 ng BEQ m^{-3}. Fig. 2a shows a high correlation coefficient ($r^2 = 0.98$, $n = 18$, $p << 0.0001$) between the results of the DR-cell assay and HRGC–HRMS analysis, and the slope of the regression line was 4.10 for flue gas from hazardous waste incineration.

For medical waste incineration samples, the I-TEQ values ranged from 0.17 to 12 ng I-TEQ N m^{-3}, and the BEQ values ranged from 0.71 to 93 ng BEQ m^{-3}. Fig. 2b shows a high correlation coefficient ($r^2 = 0.95$, $n = 20$, $p << 0.0001$) between the two methods, and the slope of the regression line was 6.07 for flue gas from medical waste incinerators. The current emission limit for medical waste incinerators in China is 0.5 ng I-TEQ N m^{-3} (MEP, 2001), which is higher than the EU legal limit of 0.1 ng I-TEQ N m^{-3}. This study reveals that 6 of 18 samples had emission levels above the current standard in China.

For iron ore sintering samples, the I-TEQ values ranged from 0.01 to 4.37 ng I-TEQ N m^{-3}, and the BEQ values ranged from 0.05 to 23.52 ng BEQ m^{-3}. Fig. 2c also shows a high correlation coefficient ($r^2 = 0.98$, $n = 21$, $p << 0.0001$) between the two